Uncertainty analysis of a fiducial-aided calibration and positioning system for precision manufacturing of optical freeform optics

Wang, S.X.[1], Cheung, C.F.[1*] and Ren, M.J.[2]

[1]State Key Laboratory of Ultra-precision Machining Technology, Department of Industrial and Systems Engineering, The Hong Kong Polytechnic University, Hung Hom, Kowloon, Hong Kong, China.

[2]Robotics Institute, School of Mechanical Engineering, Shanghai Jiao Tong University, Shanghai, China.

E-mail: **Benny.Cheung@polyu.edu.hk*

Abstract

Achieving high form accuracy of optical freeform surfaces in machining is extremely difficult due to their geometric complexity. A positioning or repositioning process is necessary for fabricating optical freeform surfaces during the machining and measuring processes. The concept of fiducial-aided calibration and positioning (FACP) has been developed to provide high-precision relative position data among different coordinate frames to minimize the repositioning errors. This paper attempts to establish an uncertainty analysis model to evaluate the uncertainty and reliability of the FACP method. Firstly, two kind of most used configurations of the FACP systems which are available for carrying out experiments both in the machining and measuring machines are designed with consideration of four main factors. Secondly, a linear transforming model is developed to connect the different coordinate fames among the machine tool, on-machine measuring system and off-machine measurement instrument with high precision. Then all the uncertainties associated in the FACP method are considered and a modified chi-square technique is applied to identify the relationship of these uncertainties. Experimental works have been conducted on two machine tools with different on-machine probing system. The results show that the transformation uncertainty is relatively very small in the proposed linear transforming model, but the final accuracy of the fiducial-aided calibration and positioning system is sensitive to the measurement results obtained from the on-machine measuring system.

Keywords: uncertainty, fiducials, freeform surface, positioning accuracy

List of abbreviations

FACP	Fiducial-aided calibration and positioning
CAD	Computer-Aided Design
FA-CAD	Fiducial-aided CAD

CMM	Coordinate measuring machine
Mcf	machining coordinate frame
Rcf	reference coordinate frame
GUM	Guide to the Uncertainty Analysis of Measurement
PSD	pooled standard deviation
RMS	root mean square

1. Introduction

Due to the excellent optical performance of complex optical freeform surfaces [1], they have received a lot of attention. The accuracy of these surfaces is very important regarding their applications and poses a lot of challenges in the fabrication of freeform surfaces in the manufacturing cycle, such as challenges in repositioning, error compensation and surface evaluation. Currently, there are many approaches for positioning or repositioning an optical freeform surface both in the fabricating and measuring processes such as techniques of on-machine trigger probe sensor [2], laser probe and fringe deflectometry system [3]. One of the common features of these techniques is the high precision of the relative positions among different coordinate frames making use of an on-machine system. Considering the rapid development of the on-machine measurement technique [4], it is a promising approach for the purpose of meeting the high requirements of manufacturing precision optical freeform surfaces. However, it is still difficult to align the machined surfaces to the nominal surface model due to the lack of references on the freeform surface. Zhang et al. [2, 3] explored two methods that combined the measured results of on-machine measurement with a contact or non-contact sensor with the off-machine coordinate measuring machine (CMM) to carry out error compensation. These methods are not only limited by the accuracy of the machined surface, but are also sensitive to the accuracy of the on-machine measurement instruments, even though great success has been achieved. As a result, a new method is explored in order to ensure the accuracy in the positioning of the machined surface.

Apart from the positioning techniques, the accuracy of the manufacturing machines is also vital to ensure the application of freeform surfaces. To improve the machining accuracy, the geometric error and thermal effects have been widely investigated. Some indirect measurement methods such as ball bars [5-7], R-test[8], and laser tracker [9] have been proposed based on modeling rigid body kinematics to correct the geometric error. However, these methods usually need a large number of measured points [10] which are time-consuming, and errors in the setup are also inevitable. To reduce the thermal effect, some researchers have built error models using various techniques, such as artificial neural network, grey model and finite element method [11]. Although many of these studies have achieved a certain level of success, the developed models still had limited applicability because of the various working environments [12]. Furthermore, it is a tedious task to fully characterize the working volume of the manufacturing machines in a thermal compensation or geometric error correction model. These challenges include, but are not limited to, lack of accuracy and robustness in the mathematical model, determining the positions of the sensor for measuring independent errors, uncertainty of the thermal expansion, and expensive and time-consuming process.

In order to improve the accuracy of 3D coordinate transformation, there are also a lot of publications in this field. Yan et.al [13]established a sensitive matrix to figure out the transforming errors and

measuring errors that hindered in the measured points. This approach may be limited by the measured points which could not represent the surface adequately. Ren [14]proposed a weighted least squares method to evaluate the coordinate transformation. They claimed that their method had less calculation and reduced measurement cost effectively. However, this method may be limited by its relative high transformation uncertainty which was great at several hundred micrometers.

In this paper, the fiducial-aided calibration and positioning system is presented to compensate for the errors of the machine tool in a different way. This method makes use of fiducials and their configuration to determine the relative accuracy between the reference system and the machine tool.

2. Fiducial-aided calibration and positioning system

In the real manufacturing cycle, relative errors including those between the workpiece and the tool tip and those between the on-machine measuring system and the off-machine measurement instrument are inevitable due to thermal expansion and volumetric positioning errors. Various techniques, such as ball-bar, laser interferometry and rigid body kinematics have been explored to describe and identify each error source. This is often a complex and challenging task because of the complexity of the machine tools in terms of geometric and thermal models.

The proposed fiducial-aided calibration and positioning system is considered a promising approach to address the error correction issue compared with other approaches which are mostly used to find the bias between the workpiece and the tool tips. Firstly, the measurement errors and machining errors caused by any of the error sources are not identified independently, but the integrated effect of errors is explored. In addition, there is no need to build any thermal or rigid body kinematic model to describe the whole volume of the machine tool. Using the measured information of the fiducials in the machining environment and fitting them to the position of the fiducial in fiducial-aided CAD (FA-CAD) which is generated in a high-precision measurement instrument (i.e. coordinate measuring machine), the fiducial-aided calibration system provides a novel approach to calibrate the cumulative errors stemming from known and unknown error sources. Hence, the compensation of the deviation is accomplished by modifying the tool path of the machine tool. It is interesting to note that this method can calibrate the working region for a specific workpiece at the time when the machining is taking place. Furthermore, the fiducial-aided calibration and positioning system is portable for any machine configuration on the condition that the FA-CAD is designed appropriately according to the characteristics of the measuring and machine tools.

In this study, the fiducial-aided calibration and positioning system was usually used to manufacture low-volume manufacturing such as small optical components in precision and ultra-precision machine tools with an on-machine measurement device. This method can also be used to manufacture large monolithic components by using the information both from local and global accuracies of the fiducials. Commercially, the available standard spheres are used in the proposed system.

2.1 Configuration of the fiducial-aided calibration and positioning system

The limitation in the machining and measuring of freeform surfaces is that they lack intrinsic surface properties. The built system should not only have the ability to provide the features (i.e. positions of the workpiece) of the designed surface and machined surface, but also be capable of providing more

information about the machine tool where the machining process is undertaken to address the problem of hidden geometric errors of the on-machine measurement system [15]. This paper attempts to consider four main factors in the design process of the fiducial-aided fixture:

1) There are at least three non-collinear fiducials to provide the position information.
2) Distribution of the fiducials should provide 3D volume information and also should avoid any collisions in the measuring and machining process.
3) The time for measuring fiducials should be minimized with a minimum number of probing elements.
4) Distribution of the fiducials is reconfigurable for different designed optical surfaces.

Limited previous research work has drawn attention to the design of such kind of artifacts. Fig. 1 shows examples of configurations.

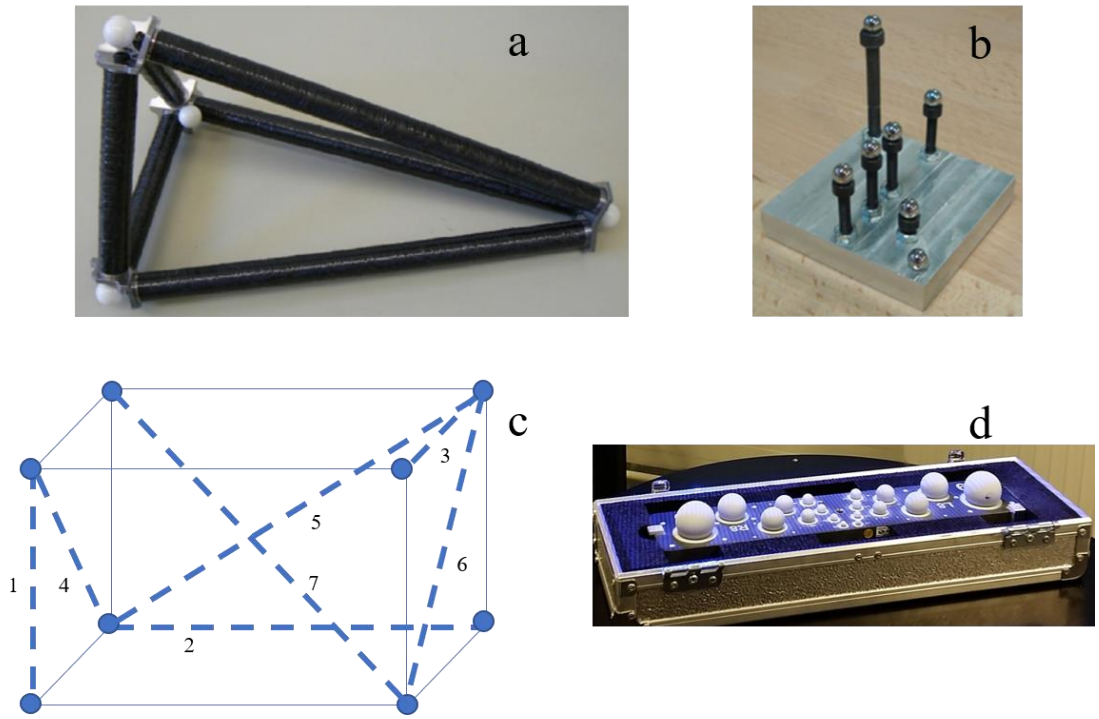

Fig.1 Examples of the configuration of the artifacts (a) small tetrahedron artifacts [16] (b) in-line and diagonal ball configuration [17] (c) VDI/VDE 2634 2014[18] (d) Calibration etalon for optical scanners [19]

These artifacts were mostly used either in the measurement process for the verification tests so as to determine the spacing errors or for calibrating and testing the performance of the CMM. None of them are applicable to the machining process with the consideration of the working conditions of the machine being used.

Motivated by the designed artifacts and combined with the four main factors in this study, two suitable configurations of the fiducial-aided fixture using standard balls were explored as shown in Fig. 2. The ball fiducials were mounted around the edges of the square or circular fixture. The fiducials were connected with rods with different heights which ranged in the working volume of the machined workpiece. In addition, the number of the fiducials should be no more than eight according to the principle in VDI/VDE 2634. The cylindrical artifact was designed for the workpiece that rotates with the

spindle and the square type is suitable for other machine tools in which the workpiece only moves along the axes of the device.

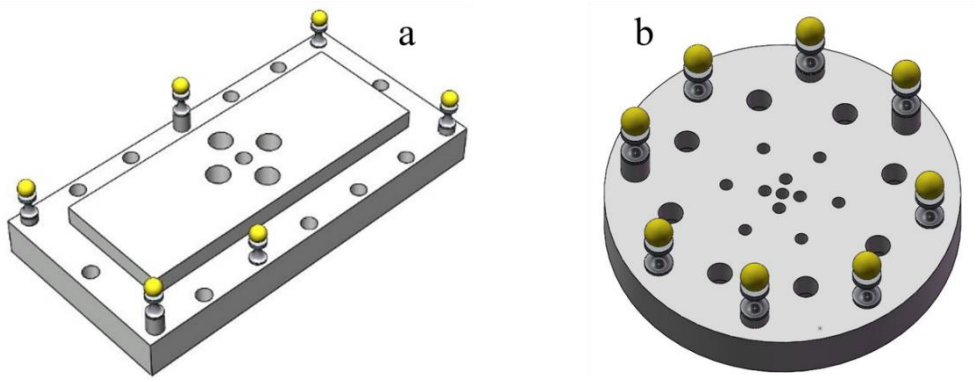

Fig. 2 Two suitable configurations of the fiducial-aided fixture with standard balls (a) Square-shaped fixture (b) Cylindrical artifact

2.2 Algorithm of the fiducial-aided calibration and positioning system

The proposed fiducial-aided calibration and positioning system consists of five key modules as shown in Fig. 3. Firstly, a fiducial-aided fixture was designed to meet the requirements of the designed surface, the shape of the workpiece and also the characteristics of the machine tools of interest. Besides, it is assumed that the workpiece is an arbitrarily shaped prismatic workpiece assembled in the fiducial-aided fixture where the six dimensions need to be considered. As a result, the material of the fixture and blank which may cause deformation at the time of interest are under consideration.

In order to fully obtain the information during the machining process, the number of fiducials and their distribution were optimized. Secondly, a fiducial-aided CAD was generated by integrating the best fitted designed surface (CAD) to the fiducial-aided fixture with the measured fiducials in a high-precision machine (i.e. CMM). Alignment of the on-machine measurement data measured in the machining coordinate frame (Mcf) with the FA-CAD established in the reference coordinate frame (Rcf) is the key input of the calibration and positioning algorithm. In other words, the proposed method and algorithm only need to transfer the points of the fiducials between Mcf and Rcf and to determine the parameters used to calculate the transformation matrix on each pair of fiducials. The output is used to generate a new error compensation tool path in the manufacture module. Then the machined surface and the fiducials can be measured and evaluated with the aid of information in the FA-CAD.

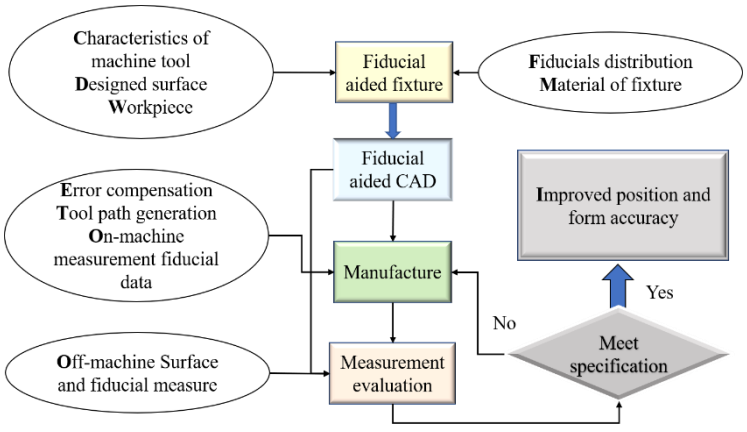

Fig. 3 Flow chart of the fiducial-aided calibration and positioning system

The relationship between the measured points in Mcf and points in Rcf is defined by Eq. (1):

$$\begin{aligned} X_c &= D_1 X_{ri} + D_2 Y_{ri} + D_3 Z_{ri} + A_x \\ Y_c &= D_4 X_{ri} + D_5 Y_{ri} + D_6 Z_{ri} + A_y \\ Z_c &= D_7 X_{ri} + D_8 Y_{ri} + D_9 Z_{ri} + A_z \end{aligned} \tag{1}$$

where (X_c, Y_c, Z_c) are the calculated points from the built reference points (X_{ri}, Y_{ri}, Z_{ri}) in Rcf. $D_1 \sim D_9, A_x \sim A_z$ are the fitted parameters

that can be found by the modified chi-squared method as defined by Eq. (2):

$$\begin{aligned} \chi^2 = & \frac{1}{3N-8}\sum_{i=1}^{N}(X_{mi} - D_1 X_{ri} + D_2 Y_{ri} + D_3 Z_{ri} + A_x) \\ & + \frac{1}{3N-8}\sum_{i=1}^{N}(Y_{mi} - D_4 X_{ri} + D_5 Y_{ri} + D_6 Z_{ri} + A_y) \\ & + \frac{1}{3N-8}\sum_{i=1}^{N}(Z_{mi} - D_7 X_{ri} + D_8 Y_{ri} + D_9 Z_{ri} + A_z) \end{aligned} \tag{2}$$

where (X_{mi}, Y_{mi}, Z_{mi}) is the measured points in Mcf. N is the total number of fiducials with more than three non-collinear fiducials. In order to find the best fitted parameters, the partial differentiation of Eq. (2) with respect to each of the 12 parameters should be set to zero. Then the parameters **M=** $[D_1 \sim D_9, A_x \sim A_z]^T$ can be solved by Eq. (3):

$$\mathbf{D} \cdot \mathbf{M} = \mathbf{R} \tag{3}$$

where $\mathbf{D}$ is a 12×12 matrix and $\mathbf{R}$ is a column vector such that Eq. (3) can be rewritten as Eq. (4):

$$\begin{bmatrix} x_r^2 & x_r y_r & x_r z_r & & & & & & & x_r & & \\ x_r y_r & y_r^2 & y_r z_r & & & & & & & y_r & & \\ x_r z_r & y_r z_r & z_r^2 & & & & & & & z_r & & \\ 0 & 0 & 0 & x_r^2 & x_r y_r & x_r z_r & & & & & x_r & \\ 0 & 0 & 0 & x_r y_r & y_r^2 & y_r z_r & & & & & y_r & \\ 0 & 0 & 0 & x_r z_r & y_r z_r & z_r^2 & & & & & z_r & \\ 0 & 0 & 0 & 0 & 0 & 0 & x_r^2 & x_r y_r & x_r z_r & & & x_r \\ 0 & 0 & 0 & 0 & 0 & 0 & x_r y_r & y_r^2 & y_r z_r & & & y_r \\ 0 & 0 & 0 & 0 & 0 & 0 & x_r z_r & y_r z_r & z_r^2 & & & z_r \\ x_r & y_r & z_r & & & & & & & N & & \\ & & & x_r & y_r & z_r & & & & & N & \\ & & & & & & x_r & y_r & z_r & & & N \end{bmatrix} \begin{bmatrix} D_1 \\ D_2 \\ D_3 \\ D_4 \\ D_5 \\ D_6 \\ D_7 \\ D_8 \\ D_9 \\ A_x \\ A_y \\ A_z \end{bmatrix} = \begin{bmatrix} x_r x_m \\ y_r x_m \\ z_r x_m \\ x_r y_m \\ y_r y_m \\ z_r y_m \\ x_r z_m \\ y_r z_m \\ z_r z_m \\ x_m \\ y_m \\ z_m \end{bmatrix} \tag{4}$$

where the $\sum$ and the subscript are dropped, for example, $x_r = \sum_{i=1}^{N} X_{ri}$, $x_r^2 = \sum_{i=1}^{N} X_{ri}^2$ and $x_r y_r = \sum_{i=1}^{N}(X_{ri} Y_{ri})$.

Eq. (4) can be easily solved, for example, Eq. (5) shows one result of the parameters,

$$
\begin{aligned}
D_1 = \{ & N\sum x_r x_m (\sum z_r y_r)^2 - (\sum z_r)\sum y_r x_m \sum x_r y_r + \sum z_r^2 \sum x_r x_m \sum y_r^2 - (\sum y_r)^2 \sum z_r x_m \sum x_r z_r \\
& + (\sum y_r)^2 \sum x_r x_m \sum z_r^2 - \sum x_m \sum x_r (\sum z_r y_r)^2 - N\sum y_r x_m \sum x_r z_r \sum z_r y_r - N\sum z_r x_m \sum x_r y_r \sum z_r y_r \\
& + N\sum z_r x_m \sum x_r z_r \sum y_r^2 + N\sum y_r x_m \sum x_r y_r \sum z_r^2 - N\sum x_r x_m \sum y_r^2 \sum z_r^2 + \sum x_m \sum y_r \sum x_r z_r \sum z_r y_r \\
& + \sum x_m \sum z_r \sum x_r y_r \sum z_r y_r + \sum x_r \sum y_r \sum z_r x_m \sum z_r y_r + \sum x_r \sum z_r \sum y_r x_m \sum z_r y_r - 2\sum y_r \sum z_r \sum x_r x_m \sum z_r y_r \\
& + \sum y_r \sum z_r \sum y_r x_m \sum x_r z_r + \sum y_r \sum z_r \sum z_r x_m \sum x_r y_r - \sum x_m \sum z_r \sum x_r z_r \sum y_r^2 - \sum x_r \sum z_r \sum z_r x_m \sum y_r^2 \\
& - \sum x_m \sum y_r \sum x_r y_r \sum z_r^2 - \sum x_r \sum y_r \sum y_r x_m \sum z_r^2 + \sum x_m \sum x_r \sum y_r^2 \sum z_r^2 \ \} / \\
\{ & N^* \sum x_r^2 (\sum z_r y_r)^2 - (\sum y_r)^2 (\sum x_r z_r)^2 - (\sum z_r)^2 (\sum x_r y_r)^2 - (\sum x_r)^2 (\sum z_r y_r)^2 + N\sum y^2{}_r (\sum x_r z_r)^2 \\
& + N(\sum x_r y_r)^2 \sum z_r^2 + (\sum z_r)^2 \sum x_r^2 \sum y_r^2 + (\sum y_r)^2 \sum x_r^2 \sum z_r^2 + (\sum x_r)^2 \sum y_r^2 \sum z_r^2 + 2\sum x_r \sum z_r \sum x_r z_r \sum z_r y_r \\
& + 2\sum x_r \sum z_r \sum x_r y_r \sum z_r y_r + 2\sum y_r \sum z_r \sum x_r y_r \sum x_r z_r - 2\sum y_r \sum z_r \sum x_r^2 \sum z_r y_r - 2\sum x_r \sum z_r \sum x_r z_r \sum y_r^2 \\
& - 2\sum x_r \sum y_r \sum x_r y_r \sum z_r^2 - 2N\sum x_r y_r \sum x_r z_r \sum z_r y_r - N\sum x_r^2 \sum y_r^2 \sum z_r^2 \ \}
\end{aligned}
\tag{5}
$$

The calculated 12 parameters contain all the combined effects for errors resulting from the measuring error sources in the manufacturing cycle such as geometric errors, probing errors and thermal errors. It is interesting to note that it is difficult to distinguish each of them independently. Furthermore, an error compensation process can be carried out by modifying the tool path of the machine tools on condition that the transforming process is reliable.

3. Uncertainty evaluation model

The achievable improvement of the machining accuracy of the FACP system depends on the error sources as shown in Fig. 4. The uncertainty analysis process follows the latest Guide to the Uncertainty Analysis of Measurement (GUM)[20].

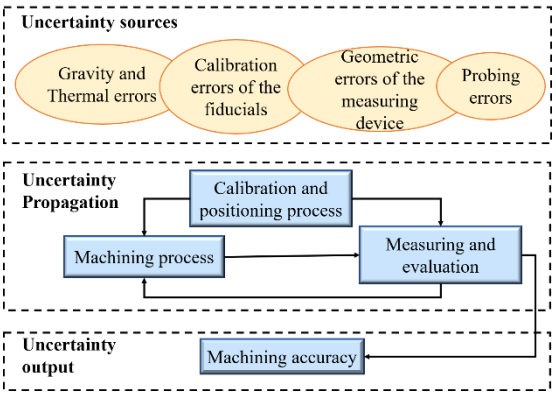

Fig. 4 Schematic diagram of uncertainty analysis of the FACP system

Several uncertainty contributors are considered including but not limited to calibration errors of the fiducials, thermal effects of the fiducial-aided fixture, measuring and machining geometric errors of the machine tools, type of fiducials, and probe errors of the measuring and on-machine measuring instruments. As aforementioned, all of these errors contribute to the combined effects for the input and output of the FACP system. Hence, there are three parts that are classified in the mathematical model, including the uncertainty of the reference data in the FA-CAD, the uncertainty in the measured points during the on-machine and evaluation measurement processes, and the uncertainty in the propagation (i.e. coordinate transformation).

3.1 Uncertainty in the FA-CAD

According to the generating process of the FA-CAD, the fiducials were bought on the commercial

market and measured by a high-precision measurement instrument (i.e. CMM) in a thermally controlled environment so that it is feasible to assume that there were no errors in the calibrations of the fiducials in the FA-CAD. Furthermore, the FACP is assumed to manufacture relatively small-sized workpieces which can be measured in one step. However, possible uncertainty occurs when the relative positions between the fiducials and CAD are changed due to gravity affecting the different positions of the fixture. For example, the fiducial-aided fixture is clamped on the measuring table in a horizontal position or vertical position. The combined uncertainty is set as σ_{rX}, σ_{rY}, σ_{rZ}.

3.2 Uncertainty in the measured points

There are many error sources in the measured points under given conditions, including but not limited to the probe repeatability and accuracy, and temperature and geometric errors of the on-machine measuring system which moves with the axes of the machining equipment. The accuracy of the probe and the repeatability can be easily tested according to Mayer and Hashemiboroujeni [21] by testing the standard sphere multiple times. Furthermore, the effect of temperature can also be measured by modifying the working temperature over a range and repeatedly testing the standard sphere. As for the errors resulting from geometric errors of the machine tool, an experimental study was conducted in previous work [22, 23], in which six transforming spatial parameters, $\left[\phi, \varphi, \gamma, \delta_x, \delta_y, \delta_z\right]$, were used to find the relationship between the standard deviation of the first three rotation parameters and the last three translation parameters and the geometric errors. The results showed that transforming errors increase with increasing geometric errors ranging from 0.5 μm to 6.5 μm (standard deviation), as shown in Fig. 5.

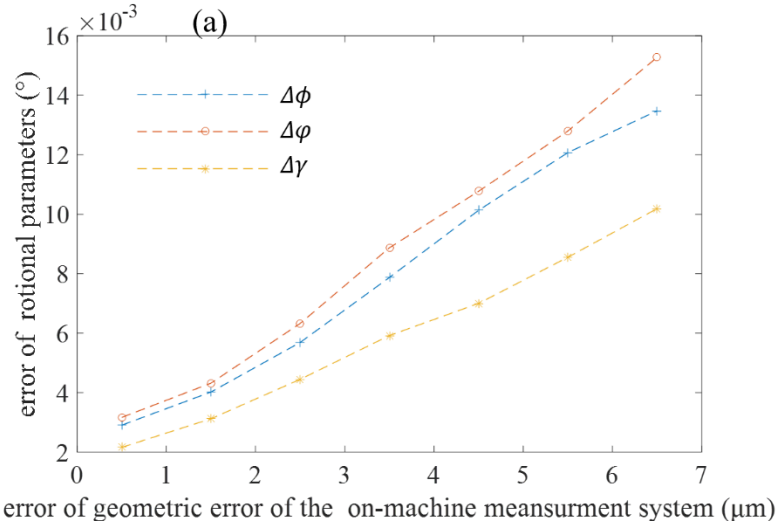

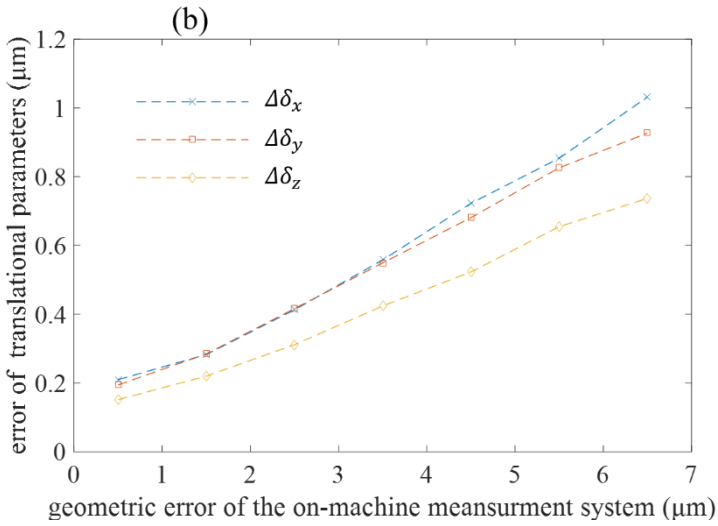

Fig. 5 The relationship between the transforming errors and the geometric errors of the machine tool. (a) error of the rotational parameters (b) error of the translational parameters. Δ denotes the deviations.

Above all, each of these three main error sources determines the uncertainty of the measured points, $\sigma_{mX},\sigma_{mY},\sigma_{mZ}$, by determining all of them using a root sum square approach.

3.3 Uncertainty in the propagation

In the mathematical model, the uncertainty sources are discussed in two areas. The first area is the uncertainty of the calculated 12 parameters. According to Eq. (4) and Eq. (5), both the measured points and the reference points in the FA-CAD determine the parameters and contribute to the uncertainty of each parameter. The uncertainty of each parameter can be determined according to Bevington et al. [24] as shown in Eq. (6) and Eq. (7):

$$\sigma^2_{D_j} = \sum_{i=1}^{N}\left\{(\frac{\partial D_j}{\partial X_{mi}})^2\sigma^2_{mX} + (\frac{\partial D_j}{\partial Y_{mi}})^2\sigma^2_{mY} + (\frac{\partial D_j}{\partial Z_{mi}})^2\sigma^2_{zY}\right\} + \sum_{i=1}^{N}\left\{(\frac{\partial D_j}{\partial X_{ri}})^2\sigma^2_{rX} + (\frac{\partial D_j}{\partial Y_{ri}})^2\sigma^2_{rY} + (\frac{\partial D_j}{\partial Z_{ri}})^2\sigma^2_{rZ}\right\} \quad (6)$$

$$\sigma^2_{A_{x,y,z}} = \sum_{i=1}^{N}\left\{(\frac{\partial A_{x,y,z}}{\partial X_{mi}})^2\sigma^2_{mX} + (\frac{\partial A_{x,y,z}}{\partial Y_{mi}})^2\sigma^2_{mY} + (\frac{\partial A_{x,y,z}}{\partial Z_{mi}})^2\sigma^2_{mZ}\right\} + \sum_{i=1}^{N}\left\{(\frac{\partial A_{x,y,z}}{\partial X_{ri}})^2\sigma^2_{rX} + (\frac{\partial A_{x,y,z}}{\partial Y_{ri}})^2\sigma^2_{rY} + (\frac{\partial A_{x,y,z}}{\partial Z_{ri}})^2\sigma^2_{rZ}\right\} \quad (7)$$

where $j=1-9$, $\sigma_{A_{x,y,z}} = (\sigma_{A_x},\sigma_{A_y},\sigma_{A_z})$. The other uncertainties stem from the algorithm in the transforming process. According to Eq. (1), Eq. (8) to Eq. (10) can be used to estimate the uncertainty of the calculated points from the measured points. On the other hand, the covariance terms of the 12 parameters must be taken into consideration due to the combination of the error sources in the mathematical model,

$$\sigma^2_{cX} = \left(\frac{\partial X_c}{\partial A_x}\right)^2\sigma^2_{A_x} + \sum_{i,j=1}^{3}\left(\frac{\partial X_c}{\partial D_i}\right)\left(\frac{\partial X_c}{\partial D_j}\right)\sigma^2_{D_iD_j} + \sum_{i=1}^{3}\left(\frac{\partial X_c}{\partial D_i}\right)\left(\frac{\partial X_c}{\partial A_x}\right)\sigma^2_{D_iA_x} \quad (8)$$

$$\sigma^2_{cY} = \left(\frac{\partial Y_c}{\partial A_y}\right)^2\sigma^2_{A_y} + \sum_{i,j=4}^{6}\left(\frac{\partial Y_c}{\partial D_i}\right)\left(\frac{\partial Y_c}{\partial D_j}\right)\sigma^2_{D_iD_j} + \sum_{i=4}^{6}\left(\frac{\partial Y_c}{\partial D_i}\right)\left(\frac{\partial Y_c}{\partial A_y}\right)\sigma^2_{D_iA_y} \quad (9)$$

$$\sigma_{cz}^2 = \left(\frac{\partial Z_c}{\partial A_z}\right)^2 \sigma_{A_z}^2 + \sum_{i,j=7}^{9}\left(\frac{\partial Z_c}{\partial D_i}\right)\left(\frac{\partial Z_c}{\partial D_j}\right)\sigma_{D_iD_j}^2 + \sum_{i=7}^{9}\left(\frac{\partial Z_c}{\partial D_i}\right)\left(\frac{\partial Z_c}{\partial A_z}\right)\sigma_{D_iA_z}^2 \tag{10}$$

where $\sigma_{D_iD_j}$ is the covariance associated with D_i and D_j at $i \neq j$, $\sigma_{D_iD_j}$ also donates the variance at $i = j$. $\sigma_{D_iA_x}$, $\sigma_{D_iA_y}$, $\sigma_{D_iA_z}$ are the covariance associated with D_i and A_x, A_y, A_z. Note that it is very complicated to determine the solutions of the above equations due to the involved covariance terms. In order to address this process, regression analysis referred to in [25] is used to derive the covariance matric. The modified chi-square function can be reformulated as:

$$\begin{aligned}\chi^2 = &\sum_{i=1}^{N}\frac{(X_{mi} - (D_1X_{ri} + D_2Y_{ri} + D_3Z_{ri} + A_x))^2}{\sigma_{mX}^2} \\ &+\sum_{i=1}^{N}\frac{(Y_{mi} - (D_4X_{ri} + D_5Y_{ri} + D_6Z_{ri} + A_y))^2}{\sigma_{mY}^2} \\ &+\sum_{i=1}^{N}\frac{(Z_{mi} - (D_7X_{ri} + D_8Y_{ri} + D_9Z_{ri} + A_z))^2}{\sigma_{mZ}^2}\end{aligned} \tag{11}$$

Similarly, the best fitted parameters can be found by setting the partial derivatives of Eq. (11) with respect to each of the 12 parameters to zeros, and formulated in matrix form as $\mathbf{D \cdot M = R}$. It is noted that the matrix $\mathbf{D}$ is different from that in Eq. (3) due to the modified Eq. (11), but there is no effect on the calculation of the 12 parameters. The terms in $\mathbf{D}^{-1}$ match the solution obtained by Eq. (6) to Eq. (7). In addition, the diagonal terms of the $\mathbf{D}^{-1}$ are variances and others are covariances. Hence, the equations obtained by partial derivative of Eq. (1) with respect to each parameter can be substituted into Eq. (8) to Eq. (10), while the final uncertainties of the transformed σ_{cX}, σ_{cY}, σ_{cZ} can be evaluated by Eq. (12) to Eq. (14) as follows:

$$\sigma_{cX}^2 = \sigma_{A_x}^2 + X_cY_c\sigma_{D_1D_2}^2 + X_cZ_c\sigma_{D_1D_3}^2 + Y_cZ_c\sigma_{D_2D_3}^2 + X_c\sigma_{D_1A_x}^2 + Y_c\sigma_{D_2A_x}^2 + Z_c\sigma_{D_3A_x}^2 + X_c^2\sigma_{D_1}^2 + Y_c^2\sigma_{D_2}^2 + Z_c^2\sigma_{D_3}^2 \tag{12}$$

$$\sigma_{cY}^2 = \sigma_{A_y}^2 + X_cY_c\sigma_{D_4D_5}^2 + X_cZ_c\sigma_{D_4D_6}^2 + Y_cZ_c\sigma_{D_5D_6}^2 + X_c\sigma_{D_4A_y}^2 + Y_c\sigma_{D_5A_y}^2 + Z_c\sigma_{D_6A_y}^2 + X_c^2\sigma_{D_4}^2 + Y_c^2\sigma_{D_5}^2 + Z_c^2\sigma_{D_6}^2 \tag{13}$$

$$\sigma_{cZ}^2 = \sigma_{A_z}^2 + X_cY_c\sigma_{D_7D_8}^2 + X_cZ_c\sigma_{D_7D_9}^2 + Y_cZ_c\sigma_{D_8D_9}^2 + X_c\sigma_{D_7A_z}^2 + Y_c\sigma_{D_8A_z}^2 + Z_c\sigma_{D_9A_z}^2 + X_c^2\sigma_{D_7}^2 + Y_c^2\sigma_{D_8}^2 + Z_c^2\sigma_{D_9}^2 \tag{14}$$

4. Experimental verification

In order to test the fiducial-aided calibration and positioning system, two experiments were conducted on two pieces of machining equipment: a three-axis CNC precision machine (MIKRON UCP 600 Vario RTT， including three translational axes, -x, -y, -z axes) and a five-axis CNC ultra-precision machine (Precitech Freeform 705, including three translational axes and two rotary axes, -B, -C axes). The first is equipped with a touch probe but the other has a developed laser probe [20].

As for the off-machine measurement, a Werth Videocheck CMM with a 2 mm diameter touch trigger probe was used. The CMM possesses length measurement uncertainty with U = (0.15 + L/400, L in mm) μm, and the probing error with u = 0.2 μm. The operations were carried out in a clean room and thermally controlled environment (± 0.2°).

The repeatability of the probing system was tested where a $\varnothing 9.997$ mm standard sphere was measured repeatedly. Table 1 shows the obtained pooled standard deviation (PSD) results of measurement repeatability of all the probing systems.

Table 1. PSD values of the probing systems

Direction	x	y	z	Overall
PSD (μm) of Precitech	0.36	0.41	0.25	0.34
PSD (μm) of UCP 600	0.92	0.94	0.84	0.90

According to the mentioned principles of configuration of the fiducial-aided system, two kinds of configurations (i.e. type C1 and type C2) of the fiducial-aided fixture (see Fig. 6) were designed to be conducted in different experiments in the precision milling machine tool and ultra-precision raster milling machine.

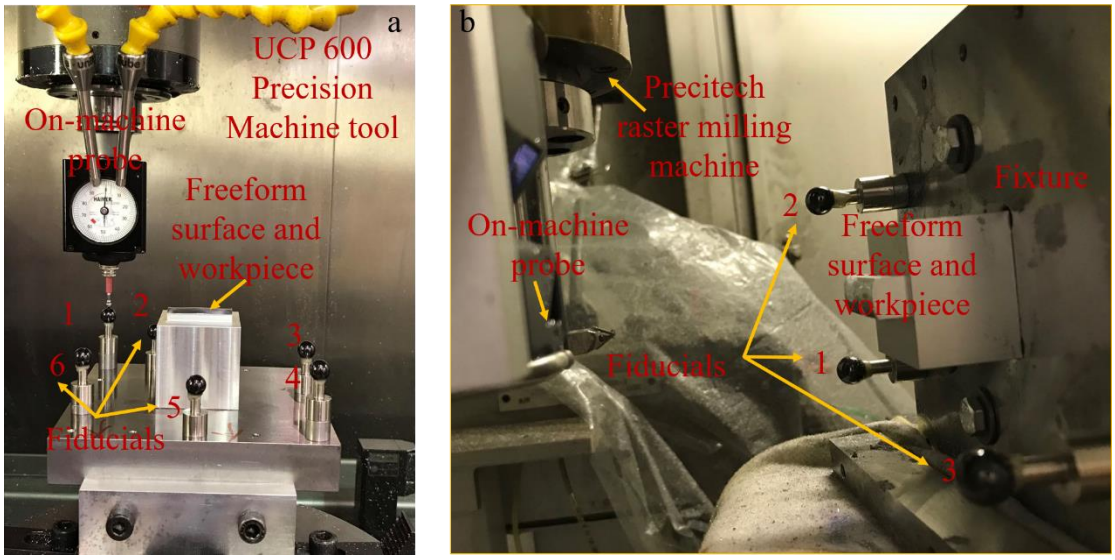

Fig. 6 Two configurations of the designed fiducial-aided fixture for two different machine tools: (a) application in the UCP 600 precision machine (b) used in the Precitech raster milling machine

As shown in Fig. 6(a), six fiducials which were located around the machined workpiece with different heights with consideration of tool collision and the machine kinematics of the MIKRON UCP 600. There were only three fiducials designed for the experiment on the raster milling machine tool in Fig. 6(b), not only because of the high precision of the ultra-precision machine tool, but also considering the volume error of the developed on-machine measuring device.

The square fixture was made of steel. All the standard balls were made of Si_3N_4. The positions and diameters of the standard sphere in the fixture were calibrated on the Werth Videocheck CMM with a fiber sensor with a 0.1 mm diameter in the thermally controlled laboratory, and the results of the diameter were 9.997 ± 0.0002 mm, which means that the uncertainties of the reference data were identified to 0.2 μm. The positions of fiducials in the reference coordinate frame (Rcf) are shown in Table 2. Moreover, the workpieces were also measured using the same sensor. A best-fitted algorithm was carried out to fit the CAD of the design surface to the measured surface so that a fiducial-aided CAD

could be generated. It is interesting to note that the errors of the best-fitted process would have no effect on the following operations.

Table 2 Positions of the fiducials in the reference coordinate frame

	Type C1			Type C2		
Fiducial	X (mm)	Y (mm)	Z (mm)	X (mm)	Y (mm)	Z (mm)
1	-59.69187	58.74985	20.10478	-60.01733	-29.99323	25.03313
2	-29.87487	59.15411	30.10673	-60.03197	29.43641	29.00935
3	60.47102	-0.53986	24.01416	59.99207	-29.80142	29.02558
4	59.48562	-59.94480	20.45916			
5	0.05844	-58.74193	30.04224			
6	-59.94523	-29.60958	25.05901			

For both of the experiments, the freeform blank was firstly assembled on the fiducial-aided fixture, then the freeform surface and the fiducials were measured by the CMM so that the positions of the measured surface and fiducials could be identified in the Rcf. Then the designed surface was best fitted into the Rcf so to replace the measured surface. According to the requirement of the machining strategy, the fiducial aided fixture was firstly mounted on the machine tool and then the fiducials was measured by the on-machine measurement instrument.

Once the positions of the fiducials were obtained, the developed algorithm was applied to obtain the matrix $\mathbf{D}^{-1}$, as shown in Eq. (15) and Eq. (16) for type C1 and C2 respectively.

$$\mathbf{D}^{-1}\_C_1 \div (e-10) =$$

$$\begin{bmatrix}
0.0429 & 0.0208 & -0.0645 & 0 & 0 & 0 & 0 & 0 & 0 & -1.29 & 0 & 0 \\
0.0208 & 0.0423 & -0.0313 & 0 & 0 & 0 & 0 & 0 & 0 & -0.466 & 0 & 0 \\
-0.0645 & -0.0313 & 4.98 & 0 & 0 & 0 & 0 & 0 & 0 & 124 & 0 & 0 \\
0 & 0 & 0 & 2.16 & 1.05 & -3.24 & 0 & 0 & 0 & 0 & -65 & 0 \\
0 & 0 & 0 & 1.05 & 2.13 & -1.57 & 0 & 0 & 0 & 0 & -23.5 & 0 \\
0 & 0 & 0 & -3.24 & -1.57 & 250 & 0 & 0 & 0 & 0 & 6230 & 0 \\
0 & 0 & 0 & 0 & 0 & 0 & 0.0271 & 0.0131 & -0.0406 & 0 & 0 & -0.814 \\
0 & 0 & 0 & 0 & 0 & 0 & 0.0131 & 0.0267 & -0.0197 & 0 & 0 & -0.294 \\
0 & 0 & 0 & 0 & 0 & 0 & -0.0406 & -0.0197 & 3.14 & 0 & 0 & 78.1 \\
-1.29 & -0.466 & 124 & 0 & 0 & 0 & 0 & 0 & 0 & 3170 & 0 & 0 \\
0 & 0 & 0 & -65 & -23.5 & 6230 & 0 & 0 & 0 & 0 & 159000 & 0 \\
0 & 0 & 0 & 0 & 0 & 0 & -0.814 & -0.294 & 78.1 & 0 & 0 & 1990
\end{bmatrix} \quad (15)$$

$$\mathbf{D}^{-1}\_C_2 \div (e-15) =$$

$$\begin{bmatrix}
0.0268 & 0.0536 & -0.643 & 0 & 0 & 0 & 0 & 0 & 0 & 19.3 & 0 & 0 \\
0.0536 & 0.107 & -1.28 & 0 & 0 & 0 & 0 & 0 & 0 & 38.6 & 0 & 0 \\
-0.643 & -1.28 & 15.4 & 0 & 0 & 0 & 0 & 0 & 0 & -463 & 0 & 0 \\
0 & 0 & 0 & 0.00281 & 0.00561 & -0.0673 & 0 & 0 & 0 & 0 & 2.02 & 0 \\
0 & 0 & 0 & 0.00561 & 0.0112 & -0.135 & 0 & 0 & 0 & 0 & 4.04 & 0 \\
0 & 0 & 0 & -0.0673 & -0.135 & 1.62 & 0 & 0 & 0 & 0 & -48.5 & 0 \\
0 & 0 & 0 & 0 & 0 & 0 & 00.247 & 0.0495 & -0.5.93 & 0 & 0 & 17.8 \\
0 & 0 & 0 & 0 & 0 & 0 & 0.0495 & 0.0989 & -1.19 & 0 & 0 & 35.6 \\
0 & 0 & 0 & 0 & 0 & 0 & -0.593 & -1.19 & 14.2 & 0 & 0 & -427 \\
19.3 & 38.6 & -463 & 0 & 0 & 0 & 0 & 0 & 0 & 13900 & 0 & 0 \\
0 & 0 & 0 & 2.02 & 4.04 & -48.5 & 0 & 0 & 0 & 0 & 1450 & 0 \\
0 & 0 & 0 & 0 & 0 & 0 & 17.8 & 35.6 & -427 & 0 & 0 & 12800
\end{bmatrix} \quad (16)$$

Then the obtained variances and covariance were substituted into Eqs. (12) − (14), and the final uncertainties in three directions were calculated as shown in Table 3.

Table 3 Uncertainties of the calculated results using the matrix stemming from the two experiments

	C1 (touch probe)						C2 (laser probe)		
Fiducials	1	2	3	4	5	6	1	2	3
σ_{x_c} (μm)	1.92	2.32	2.14	1.92	2.32	2.14	0.032	0.041	0.043
σ_{y_c} (μm)	2.63	3.14	2.82	2.63	3.14	2.82	0.011	0.012	0.012
σ_{z_c} (μm)	0.34	0.41	0.36	0.34	0.40	0.37	0.033	0.034	0.036

Once the errors of the calculated points were obtained, the new tool path for machining the freeform surface were generated with consideration of error compensation. In the evaluation of the freeform surface, the fiducials serve as intrinsic surface features to carry out the rough matching process. The 3D error (in the z direction) topography of the two machined surfaces after error compensation is shown in Fig. 7.

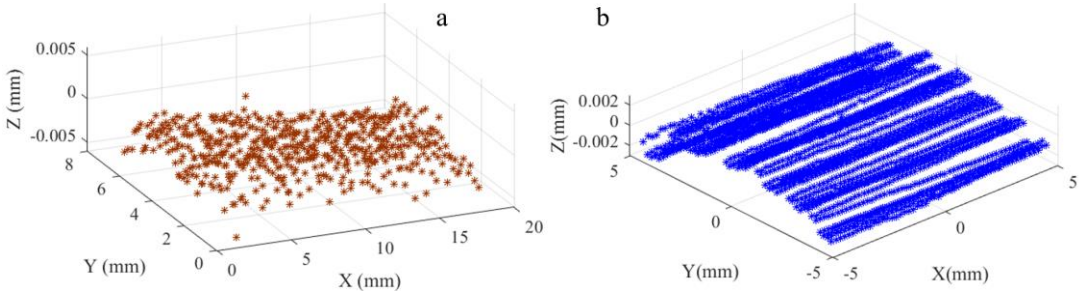

Fig. 7 3D error topographies for the surfaces in the two machines after error compensation. (a) F-theta surface, $z = (-1/250)x^2 + (1/92000)x^4 - (1/25)y^2,\ x \in [0,18], y \in [0,7.5]$ (b) Sinusoidal surface, $z = \sin(0.2x) + \cos(0.2y), x \in [-5,5], y \in [5,5]$

The root mean square (RMS) values of the form errors are always used to characterize the form deviation. As shown in Fig. 6, the RMS values of the F-theta lens and sinusoidal surface processed on

the precision and ultra-precision machine tool were about 2.48 μm in and 0.84 μm, respectively.

5. Discussion

In the FACP system, there are four critical uncertainties which were described in the above sections, including the uncertainty resulting from reference data ($\sigma_{rX},\sigma_{rY},\sigma_{rZ}$), measured data ($\sigma_{mX},\sigma_{mY},\sigma_{mZ}$), the calculated data ($\sigma_{cX},\sigma_{cY},\sigma_{cZ}$) as well as the parameters used in the mathematical model (D_i , $\sigma_{D_iD_j}$, $\sigma_{A_x},\sigma_{A_y},\sigma_{A_z}$, $\sigma_{D_iA_x}$, $\sigma_{D_iA_y}$, $\sigma_{D_iA_z}$). According to the measured data in different on-machine measurement systems with different accuracies, the uncertainties of the best fitted values are very small and up to 10e-7 mm as shown in Eq. (15) and Eq. (16). In most cases, the reference data have relatively low uncertainties compared with those of the measured data. However, the fiducials fixture that serves as reference data may be affected by the gravity and thermal ranges in different working environments. Hence, the combined uncertainties also need to be considered in the actual measurement by testing the fiducials and their distribution. In the present study, a total of 0.2 μm was estimated as the final uncertainty in three directions. It is worthy of note that the material of the fixture and the heights of the fiducials should be modified if the uncertainty of the measured data is larger than the acceptable level.

In the final calculated data, the combined uncertainties were estimated with consideration of the other three uncertainty sources. As shown in Table 3, the uncertainties are sensitive to different on-machine measurement systems. In the touch probe system, the uncertainties were up to 2.32 μm, 3.14 μm, and 0.41 μm in the x, y, and z directions, respectively. However, uncertainties of the laser system are only 1% compared with those in touch probe system, which ranges from only 0.011 μm to 0.043 μm. This is mainly due to the different geometric errors of the associated machine tool in the working volume. It is clear that these geometric errors also have a large influence on the calculation of the 12 parameters which can be seen from their uncertainties in Eq. (15) to Eq. (16). On the other hand, the accuracy of the probes is also considered to be a contributor.

On the contrary, in many cases, the final uncertainty of the data was determined in the design process which did not exceed 10% of the part tolerance [25]. As a result, it is also possible to decide how to choose an on-machine measurement instrument based on solving Eq. (6) and Eq. (7) and obtaining the uncertainty of the measured data ($\sigma_{mX},\sigma_{mY},\sigma_{mZ}$).

Regarding the accuracy of the machined surfaces, the expected results in terms of the RMS values in the z direction were around the scale of the uncertainties obtained in the mathematical model. According to Fig.7, the error of the machined F-theta lens in the z direction was larger than that in the mathematical model shown but it agreed reasonably well with the combined uncertainties, ($\sigma_{x_c},\sigma_{y_c},\sigma_{z_c}$), as shown in Table 3. In the ultra-precision machine tool, the performance of the sinusoidal surface was also not good although the RMS values were acceptable (at the sub-micrometer level). One possible reason was the configuration of the on-machine probing system. The identification of the relative position between the probe tip and the cutting tools also introduced uncertainties.

It interesting to note that the uncertainty in the measured data can also be limited if the uncertainty of the reference data and final calculated data are determined. By substituting Eqs. (6) – (7) into Eqs. (12) – (14), the measured uncertainty in the machine part can be determined by Eqs. (17) – (19) without

considering the covariances:

$$\sigma_{mX}^2 = \frac{\sigma_{cX}^2 - \sigma_{rX}^2 (X_c^2 \sum_{i=1}^{N} (\frac{\partial D_1}{\partial X_{ri}})^2 + Y_c^2 \sum_{i=1}^{N} (\frac{\partial D_2}{\partial X_{ri}})^2 + Z_c^2 \sum_{i=1}^{N} (\frac{\partial D_3}{\partial X_{ri}})^2 + \sum_{i=1}^{N} (\frac{\partial A_x}{\partial X_{ri}})^2)}{(X_c^2 \sum_{i=1}^{N} \frac{\partial D_1}{\partial X_{ri}})^2 + Y_c^2 \sum_{i=1}^{N} \frac{\partial D_1}{\partial X_{ri}})^2 + Z_c^2 \sum_{i=1}^{N} \frac{\partial D_1}{\partial X_{ri}})^2 + \sum_{i=1}^{N} \frac{\partial A_x}{\partial X_{ri}})^2} \tag{17}$$

$$\sigma_{mY}^2 = \frac{\sigma_{cY}^2 - \sigma_{rY}^2 (X_c^2 \sum_{i=1}^{N} (\frac{\partial D_4}{\partial Y_{ri}})^2 + Y_c^2 \sum_{i=1}^{N} (\frac{\partial D_5}{\partial Y_{ri}})^2 + Z_c^2 \sum_{i=1}^{N} (\frac{\partial D_6}{\partial Y_{ri}})^2 + \sum_{i=1}^{N} (\frac{\partial A_y}{\partial Y_{ri}})^2)}{(X_c^2 \sum_{i=1}^{N} \frac{\partial D_4}{\partial Y_{ri}})^2 + Y_c^2 \sum_{i=1}^{N} \frac{\partial D_5}{\partial Y_{ri}})^2 + Z_c^2 \sum_{i=1}^{N} \frac{\partial D_6}{\partial Y_{ri}})^2 + \sum_{i=1}^{N} \frac{\partial A_y}{\partial Y_{ri}})^2} \tag{18}$$

$$\sigma_{mZ}^2 = \frac{\sigma_{cZ}^2 - \sigma_{rZ}^2 (X_c^2 \sum_{i=1}^{N} (\frac{\partial D_7}{\partial Z_{ri}})^2 + Y_c^2 \sum_{i=1}^{N} (\frac{\partial D_8}{\partial Z_{ri}})^2 + Z_c^2 \sum_{i=1}^{N} (\frac{\partial D_9}{\partial Z_{ri}})^2 + \sum_{i=1}^{N} (\frac{\partial A_z}{\partial Z_{ri}})^2)}{(X_c^2 \sum_{i=1}^{N} \frac{\partial D_7}{\partial Z_{ri}})^2 + Y_c^2 \sum_{i=1}^{N} \frac{\partial D_8}{\partial Z_{ri}})^2 + Z_c^2 \sum_{i=1}^{N} \frac{\partial D_9}{\partial Z_{ri}})^2 + \sum_{i=1}^{N} \frac{\partial A_z}{\partial Z_{ri}})^2} \tag{19}$$

For example, for a $10mm \times 10mm$ optical freeform surface with a 1 *mm* height range in the *z* direction, the desired maximum final uncertainty is 0.8 μm and the uncertainty of the reference data is 0.3 μm. Four fiducials surround the workpiece in a grid pattern with *x* and *y* spacing of 10 *mm* and *z* spacing of 1 *mm*. Substituting these values into the above equations, the uncertainty in measured points is 1.5 μm. In other words, the combined uncertainty including that stemming from the machining process and on-machine measurement process cannot be larger than 1.5 μm as calculated with a root sum square method.

6. Conclusions

In this paper, an uncertainty analysis method is presented for a fiducial-aided calibration and positioning system which attempts to provide an approach to transform the accuracy of high-precision off-machine measurement equipment to the machine tool where the machining process is undertaken.

Firstly, two most suitable fiducial-aided fixtures were designed with consideration of those factors such as the characteristics of machining and measuring machine tools, measuring time and enough measured information. Then a linear mathematical model was built to connect the measured points obtained in different coordinate frame. Meanwhile, the uncertainty model in the fiducial-aided calibration and positioning system were analyzed. Some of the uncertainties such as the on-machine and off-machine measurement instruments, the relationship between the geometric error of the machine tool and the transforming error were presented. A modified chi-square technique is used to identify uncertainties from the sources and propagation. Two experiments were carried out on different machine tool with different machining and measuring accuracy. The results show that the uncertainties resulted from the linear mathematical model are very small and up to 10e-7 mm which means the transforming accuracy can be guaranteed by the developed model. However, the final calculated data indicated that the combined uncertainties are sensitive to the measurement uncertainties. The lower accuracy of the on-machine measuring system could lead to higher uncertainties, which means the accuracy of the on-machine measuring system has a large influence on the accuracy of the system. Two freeform surfaces were machined by modifying the tool path to compensate the errors in the machine tool. The root mean square value of the two freeform surfaces showed that the surface form accuracy were relatively good at micro and sub-micro level (2.48 μm and 0.84 μm in precision and ultra-precision machine tool respectively). The experimental results demonstrated that the developed transforming method and the modified chi-

square technique can easily evaluate the uncertainties in the FACP system and the achievable improvement of the form accuracy of FACP system depends on the distribution of the fiducials, and the relatively high credible relationship between the cutting tool and the probing system. Besides, the measuring device, distribution of the fiducials and measuring time can be optimized if the expected accuracy is given in the final data according to the proposed method.

Acknowledgements

The work described in this paper was fully supported by a grant from the Research Grants Council of the Government of the Hong Kong Special Administrative Region, China (Project No.: PolyU 15202814). The authors would also like to express their sincere thanks to the Research Committee of The Hong Kong Polytechnic University for their financial support of the project through a PhD studentship (project account code: RUEN).

Reference

[1] A. Bauer, E. M. Schiesser, and J. P. Rolland, "Starting geometry creation and design method for freeform optics," *Nature Communications,* vol. 9, p. 1756, 2018/05/01 2018.

[2] X. Zhang, Z. Zeng, X. Liu, and F. Fang, "Compensation strategy for machining optical freeform surfaces by the combined on-and off-machine measurement," *Optics Express,* vol. 23, pp. 24800-24810, 2015.

[3] X. Zhang, L. Jiang, and G. Zhang, "Novel method of positioning optical freeform surfaces based on fringe deflectometry," *CIRP Annals-Manufacturing Technology,* 2017.

[4] D. Li, Z. Tong, X. Jiang, L. Blunt, and F. Gao, "Calibration of an interferometric on-machine probing system on an ultra-precision turning machine," *Measurement,* vol. 118, pp. 96-104, 2018/03/01/ 2018.

[5] X. Jiang and R. J. Cripps, "A method of testing position independent geometric errors in rotary axes of a five-axis machine tool using a double ball bar," *International Journal of Machine Tools and Manufacture,* vol. 89, pp. 151-158, 2015.

[6] L. Zhong, Q. Bi, and Y. Wang, "Volumetric accuracy evaluation for five-axis machine tools by modeling spherical deviation based on double ball-bar kinematic test," *International Journal of Machine Tools and Manufacture,* vol. 122, pp. 106-119, 2017/11/01/ 2017.

[7] A. Lasemi, D. Xue, and P. Gu, "Accurate identification and compensation of geometric errors of 5-axis CNC machine tools using double ball bar," *Measurement Science and Technology,* vol. 27, p. 055004, 2016.

[8] C. Hong and S. Ibaraki, "Non-contact R-test with laser displacement sensors for error calibration of five-axis machine tools," *Precision Engineering,* vol. 37, pp. 159-171, 2013/01/01/ 2013.

[9] S. Aguado, D. Samper, J. Santolaria, and J. J. Aguilar, "Identification strategy of error parameter in volumetric error compensation of machine tool based on laser tracker measurements," *International Journal of Machine Tools and Manufacture,* vol. 53, pp. 160-169, 2012.

[10] A. Wan, L. Song, J. Xu, S. Liu, and K. Chen, "Calibration and compensation of machine tool volumetric error using a laser tracker," *International Journal of Machine Tools and Manufacture,* vol. 124, pp. 126-133, 2018.

[11] J. Yang, H. Shi, B. Feng, L. Zhao, C. Ma, and X. Mei, "Thermal error modeling and compensation for a high-speed motorized spindle," *The International Journal of Advanced*

Manufacturing Technology, vol. 77, pp. 1005-1017, 2015.

[12] L. Sun, M. Ren, H. Hong, and Y. Yin, "Thermal error reduction based on thermodynamics structure optimization method for an ultra-precision machine tool," *The International Journal of Advanced Manufacturing Technology,* vol. 88, pp. 1267-1277, 2017.

[13] Z. Yan and C.-H. Menq, "Uncertainty analysis and variation reduction of three-dimensional coordinate metrology. Part 2: uncertainty analysis," *International Journal of Machine Tools and Manufacture,* vol. 39, pp. 1219-1238, 1999.

[14] Y. Ren, J. Lin, J. Zhu, B. Sun, and S. Ye, "Coordinate transformation uncertainty analysis in large-scale metrology," *IEEE Transactions on Instrumentation and Measurement,* vol. 64, pp. 2380-2388, 2015.

[15] F. Fang, X. Zhang, A. Weckenmann, G. Zhang, and C. Evans, "Manufacturing and measurement of freeform optics," *CIRP Annals-Manufacturing Technology,* vol. 62, pp. 823-846, 2013.

[16] B. Acko, M. McCarthy, F. Haertig, and B. Buchmeister, "Standards for testing freeform measurement capability of optical and tactile coordinate measuring machines," *Measurement science and technology,* vol. 23, p. 094013, 2012.

[17] G. Moroni, S. Petrò, and W. P. Syam, "Four-axis micro measuring systems performance verification," *CIRP Annals,* vol. 63, pp. 485-488, 2014.

[18] G. mbH, " GOM Acceptance Test – Process Description, Acceptance Test according to the Guideline VDI/VDE 2634 Part 3," ed. Braunschweig, Germany, 2014.

[19] R. Mendricky, "Determination of measurement accuracy of optical 3D scanners," *MM SJ,* pp. 1565-1572, 2016.

[20] I. BIPM, I. IFCC, and I. ISO, "IUPAP, and OIML, 2008,“Evaluation of Measurement Data—Guide to the Expression of Uncertainty in Measurement,” Joint Committee for Guides in Metrology," Technical Report No. JCGM 1002008.

[21] J. Mayer and H. Hashemiboroujeni, "A ball dome artefact for coordinate metrology performance evaluation of a five axis machine tool," *CIRP Annals,* vol. 66, pp. 479-482, 2017.

[22] S. Wang, C. Cheung, M. Ren, and M. Liu, "Fiducial-aided on-machine positioning method for precision manufacturing of optical freeform surfaces," *Optics express,* vol. 26, pp. 18928-18943, 2018.

[23] S. Wang, C. Cheung, M. Ren, and M. Liu, "Fiducial-Aided Robust Positioning of Optical Freeform Surfaces," *Micromachines,* vol. 9, p. 52, 2018.

[24] P. R. Bevington, D. K. Robinson, J. M. Blair, A. J. Mallinckrodt, and S. McKay, "Data reduction and error analysis for the physical sciences," *Computers in Physics,* vol. 7, pp. 415-416, 2003.

[25] B. A. Woody, K. S. Smith, R. J. Hocken, and J. A. Miller, "A technique for enhancing machine tool accuracy by transferring the metrology reference from the machine tool to the workpiece," *Journal of manufacturing science and engineering,* vol. 129, pp. 636-643, 2007.